TABLE OF CONTENTS

Micropore formation around the ZrO_2 nanoparticles is caused by the moisture adsorbed on the surface of nanoparticles. This significantly affects the physicochemical properties of the composite separators and, by extension, the electrochemical performance of the lithium-ion batteries.
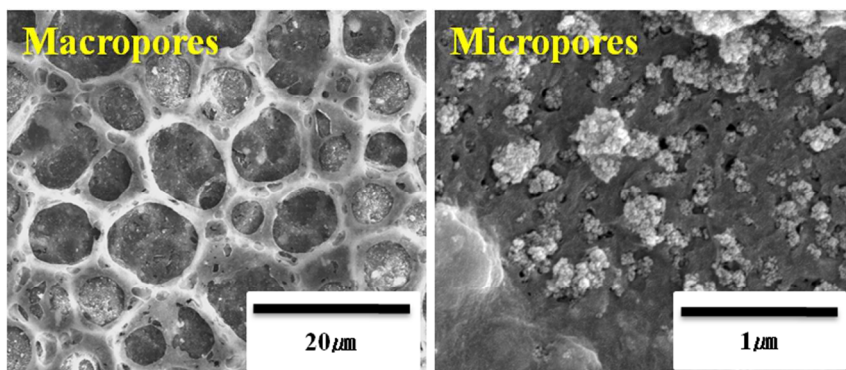
Ceramic composite separator with integrated moisturized ZrO$_2$ nanoparticles for securing electrochemical and thermal stabilities of lithium ion batteries

Ki Jae Kim, Hyuk Kwon Kwon, Min-Sik Park,* Taeeun Yim, Ji-Sang Yu and Young-Jun Kim

[a] Advanced Batteries Research Center, Korea Electronics Technology Institute, 68 Yatap-dong, Bundang-gu, Seongnam 463-816, Republic of Korea

*Corresponding Author

Tel: +82-31-789-7496, Fax: +82-31-789-7499

Email: parkms@keti.re.kr

1

ABATRACT

We introduce a ceramic composite separator prepared by coating moisturized ZrO_2 nanoparticles with a poly(vinylidene fluoride-co-hexafluoropropylene) (PVDF-12wt%HFP) copolymer on a polyethylene separator. The effect of moisturized ZrO_2 nanoparticles on the morphology and microstructure of the polymeric coating layer is investigated. A large number of micropores formed around the embedded ZrO_2 nanoparticles in the coating layer as a result of the phase inversion caused by the adsorbed moisture. The formation of micropores highly affects the ionic conductivity and electrolyte uptake of the ceramic composite separator and, by extension, the rate discharge properties of lithium ion batteries. In particular, thermal stability of the ceramic composite separator coated with the highly moisturized ZrO_2 nanoparticles (moisture content of 16000 ppm) is dramatically improved without any degradation in electrochemical performance compared to the performance of pristine polyethylene separators.

KEYWORDS

2

INTRODUCTION

In recent years, the demand for hybrid electric vehicles (HEVs) and plug-in hybrid electric vehicles (PHEVs) has increased due to the desire to reduce increased emission of greenhouse gases and consumption of fossil fuels. Lithium ion batteries (LIBs) are regarded as suitable power sources for EV applications because of their high energy and power. However, safety is still an important and serious concern in the development of LIBs for these applications. To improve the safety of these batteries, many researchers have focused on the improvement of the thermal and mechanical properties of separators.[1-4] The separator plays a key role in ensuring the safety of LIBs by preventing short circuit between the cathode and anode.[5] This implies that the separator must be a good electrical insulator and must possess good mechanical and dimensional stability as well as electrochemical stability toward electrolyte and electrode materials.[5]

Polyethylene (PE) separators have been widely used in commercial LIBs and have many advantages such as good electrochemical stability, high mechanical strength, small pore size, and thin frames.[6] Despites these properties, the poor thermal stability of PE separators is a disadvantage that needs to be resolved. When exposed to high-temperature environments, PE separators exhibit extensive thermal shrinkage and significant structural degradation, which may trigger internal short circuits in the LIBs. Consequently, the thermal stability of PE separators needs to be further improved to meet the rigorous safety standards for LIBs for EV applications.

Since the introduction of separators such as safety-reinforced separators (SRS) by LG Chem., various ceramic composite separators have been proposed for practical use in LIBs.[7-10] For example, Takemura et al. proposed a ceramic composite separator that was made of Al_2O_3 ceramic powder and a polymer binder on a PE framework and that exhibited good thermal

stability.[8] Zhang et al. also reported a CaCO$_3$-based composite separator with excellent thermal stability, in which CaCO$_3$ ceramic particles coating the separator acted as a heating-resistant material suppressing the thermal shrinkage of the separator.[9] Previous works have largely focused on the improvement of thermal properties of separators by incorporating various ceramic particles. However, the effect of the ceramic particles on the electrochemical performance of LIBs has not yet been intensively studied.

We herein propose a ceramic composite separator that is coated by a polymeric binder [poly(vinylidene fluoride-co-hexafluoropropylene) (PVdF-12wt%HFP) copolymer] and moisturized ZrO$_2$ nanoparticles. We demonstrate the structural changes of the polymer coating layer induced by the moisture adsorbed on ZrO$_2$ nanoparticles, and discuss the correlation between the microstructure of the ZrO$_2$-composite separator and its electrochemical and thermal properties. Our findings can lead to robust ceramic composite separator designs that will improve thermal stability of LIBs for EV applications.

EXPERIMENTAL DETAILS

Commercial PE separator (Asahi Korea Chemicals) and PVDF-12wt%HFP copolymer (molecular weight = 470,000) were used as a framework and polymer binder, respectively. The physical properties of ZrO$_2$ nanoparticles are shown in Table 1. The ZrO$_2$ nanoparticles were preferentially dried at 120 °C for 24 h in a vacuum oven to remove the adsorbed moisture before use. ZrO$_2$ nanoparticles were stored in a humidity chamber at 60 °C for different storage times with a relative humidity (R.H.) of 95%, to vary their moisture content. The moisture content of the as-dried ZrO$_2$ nanoparticles was increased from 100 to 3000, 6000, 15000 and 16000 ppm

after storage for 5 min, 30 min, 3 h and 24 h, respectively. The moisture content of the ZrO_2 nanoparticles was saturated beyond the storage time of 24 h. Karl Fisher titration (Metrohm 832 KF Thermoprep) was used to measure the moisture content of the ZrO_2 nanoparticles. To prepare the ZrO_2-ceramic separators, moisturized ZrO_2 nanoparticles (2.4 g) and PVDF-12wt%HFP copolymer (1.6 g) were dissolved in acetone (80 cc) at room temperature by stirring vigorously using a high-speed mixer for dispersing ZrO_2 nanoparticles in the solution. The PE separator was dipped in the coating solution and dried under an R.H. of 35% using a humidity control system. Finally, the composite separator was dried at 50 °C for 12 h in a vacuum oven to remove residual moisture before use.

The morphology and microstructure of the ZrO_2-composite separators were analyzed using a field emission scanning electron microscopy (FE-SEM, JEOL JSM-7000F). A Gurley-type densometer (Toyoseiki) was used to measure the Gurley number of the ZrO_2-composite separators. The electrolyte uptake was examined by measuring the weight of ZrO_2-composite separators with a given area before and after soaking it in a liquid electrolyte for 24 h. The uptake was then calculated using equation (1):

Electrolyte uptake (%) = $(W_f - W_i)/W_i \times 100$ (1)

where W_i and W_f are the weights of the separators before and after soaking, respectively. The thermal shrinkage was determined by measuring the dimensional change of the separators after storage at 120 °C and 150 °C for 1 h, respectively.

To measure the thermal shrinkage properties, the separators (5 cm × 5 cm in size) were stored in an oven at120 and 150 ^{o}C for 1 h. After the storage, dimensional changes of the separators were carefully measured by equation (2):

Shrinkage (%) = $(A_i - A_f) / A_i \times 100$ (2)

where A_i and A_f are the initial and final area of the separators, respectively. Thermal analysis of the PE separator and the ZrO_2-composite separators was carried out using a differential scanning calorimetry (DSC, METTLER TOLEDO) under N_2 atmosphere with a heating rate of 5 ^{o}C min^{-1}.

A 2032 coin cell was assembled by sandwiching the ZrO_2-composite separators between two Li-metal electrodes and then soaking them in a liquid electrolyte to measure ionic conductivity. The AC impedance was measured by using a Solatron 1280C over the frequency range 0.1–20,000 Hz with an AC-amplitude of 10 mV. The ionic conductivity was calculated using the relation $\sigma = d/RA$, where d and A are the thickness and area of the separators, respectively, and R is the electrolyte resistance obtained from the AC impedance test. To evaluate the electrochemical performance of the ZrO_2-composite separator, we prepared 2032 coin cells, which were composed of the separator, a $LiCoO_2$ electrode as a working electrode, and a Li-metal as a counter electrode. The cathode was prepared by coating a slurry containing lithium cobalt oxide ($LiCoO_2$, Umicore, Korea, 92wt%) as an active material, conducting agent (Super-P), and polyvinylidene fluoride binder (KF1100, Kureha, 4 wt%) dissolved in N-methyl-2-pyrrolidone (NMP) on Al foil. After coating, the cathode was dried at 120 ^{o}C for 10 h and pressed. The loading level for the cathode was 27.2 ± 0.5 mgcm^{-2}. A liquid electrolyte was composed of 1 M $LiPF_6$ in ethylene carbonate (EC) / ethyl methyl carbonate (EMC) (3 : 7 by volume, PANAX ETEC) and 3 wt% vinylene carbonate (VC) additive. The rate discharge tests were performed over 3.0–4.2 V *vs.* Li/Li$^+$ at different currents of 0.2, 0.5, 1, 2 and 3 C (1 C =

150 mA g^{-1}). The cyclic performance was examined under a constant current mode at 0.5 C from 3.0 to 4.2 V *vs.* Li/Li^{+} using a cycle tester (Maccor 8500).

RESULTS AND DISCUSSION

3.1. A ceramic composite separator using moisturized ZrO$_2$ nanoparticles

According to previously reported studies, it was generally accepted that the PVDF-12wt%HFP copolymer formed a porous structure through phase inversion when the copolymer contained a certain amount of moisture.[11-14] In other words, the moisture adsorbed on the ceramic particles would be a critical factor in determining the microstructure of the polymeric coating layer on the ceramic composite separators because of their hydrophilicity.[15,16] To prove this hypothesis, we prepared a ceramic composite separator by coating a PE separator with moisturized ZrO$_2$ nanoparticles using PVDF-12wt%HFP copolymer as a binder. Spherical ZrO$_2$ nanoparticles with a size of less than 50 nm were used in this study. The moisturized ZrO$_2$ nanoparticles have a moisture content of 3000 ppm, which can be reasonably reduced to 100 ppm after drying at 120 °C for 24 h.

To demonstrate the effects of moisture adsorbed on the ZrO$_2$ nanoparticles on the microstructure of the polymeric coating layer of the PVDF-12wt%HFP copolymer, the composite separators were prepared using both moisturized ZrO$_2$ nanoparticles (3000 ppm) and dried ZrO$_2$ nanoparticles (100 ppm). For comparison, we also prepared a composite separator coated with only PVDF-12wt%HFP copolymer without ZrO$_2$ nanoparticles. The morphology and microstructure of the as-prepared composite separators were examined using FE-SEM, as

shown in Fig. 1. A 4-µm-thick coating layer successfully formed on the surface of the PE separators after the coating process. We observed that the macropores 5–10 µm in size had formed uniformly on the separators (Fig. 1a, 1c and 1e), regardless of the addition of ZrO_2 nanoparticles and their moisture contents. Macropore formation is generally induced by the phase inversion of the PVDF-12wt%HFP copolymer, as reported by many researchers.[11-14]

Further, we found that the ZrO_2 nanoparticles were well distributed in the polymeric coating layer of the PVDF-12wt%HFP copolymer as shown in Fig. 1d and 1f. Interestingly, micropores smaller than 1 µm also formed around the ZrO_2 nanoparticles in the polymeric coating layer when the moisturized ZrO_2 nanoparticles with a moisture content of 3000 ppm were employed (Fig. 1e). In contrast, we could not find any evidence of micropore formation in the polymeric coating layer prepared with dried-ZrO_2 nanoparticles (Fig. 1d). We claimed that the moisture adsorbed on the ZrO_2 nanoparticles is mainly responsible for the formation of micropores in the polymeric coating layer.

In order to further inspect the microstructure of the polymeric coating layer induced by the moisture adsorbed on the ZrO_2 nanoparticles, we carried out air permeability and ionic conductivity measurements (Fig. 2a). The composite separator containing moisturized ZrO_2 nanoparticles showed a lower Gurley number of 309 s/100cc, compared to the separator with dried ZrO_2 nanoparticles (399 s/100cc). This indicates that the polymeric coating layer with moisturized ZrO_2 nanoparticles has a more open structure as a result of micropore formation induced by the moisture adsorbed on the ZrO_2 nanoparticles. Improved ionic conductivity of the composite separator reflects positive characteristics such as this more open structure. The composite separator containing moisturized ZrO_2 nanoparticles showed a higher ionic conductivity of 6.1×10^{-4} S cm^{-1} than the separator with dried ZrO_2 nanoparticles (3.9×10^{-4} S

cm^{-1}). The formation of micropores in the polymeric coating layer was also effective in enhancing the electrolyte uptake of the composite separators, which is a critical factor directly affecting the electrochemical performance of LIBs (Fig. 2b).

To investigate the effect of micropore formation in the ZrO$_2$-composite separator on the electrochemical performance of LIBs, the rate capabilities of the cells employing the composite separators were examined at different current densities (0.2, 0.5, 1.0, 2.0 and 3.0 C). Fig. 2c shows that, even at a high current density of 3.0 C, the composite separator containing moisturized ZrO$_2$ nanoparticles exhibited a higher capacity retention (34.4%) than the separators with dried ZrO$_2$ nanoparticles and only PVDF-12wt%HFP copolymer (capacity retentions of 23.1% and 23.0%, respectively). It seemed that the abundant micropores formed around the ZrO$_2$ nanoparticles effectively facilitated Li$^+$ migration, leading to a better rate capability. Based on those observations, we suggest that the pore structure of the polymeric coating layer of the composite separator greatly affected the electrochemical performance of the LIBs.

These results supported the fact that micropore formation around the ZrO$_2$ nanoparticles was caused by moisture adsorbed on the surface of ZrO$_2$ nanoparticles. The micropore formation significantly affected the physicochemical properties of the composite separators and, by extension, the electrochemical performance of the LIBs. Phase inversion induced by the moisture adsorbed on the ZrO$_2$ nanoparticles acted as the mechanism micropore formation. Moreover, micropore formation was a predominant factor in determining the physicochemical properties of the separator.

3.2. Effect of moisture content on the microstructure of the ZrO$_2$-composite separators

To clarify the correlation between the moisture content of the ZrO_2 nanoparticles and the microstructure of the polymeric coating layer, we prepared various moisturized ZrO_2 nanoparticles with different moisture contents by storing the ZrO_2 nanoparticles in a humid atmosphere (60 °C, R.H. 95%). The moisture content was controlled by adjusting storage time. Fig. 3 shows the morphologies of the ZrO_2-composite separators prepared using moisturized ZrO_2 nanoparticles with moisture contents of 6000, 15000 and 16000 ppm. Comparison of the morphologies of the composite separators with ZrO_2 nanoparticles and various moisture contents showed that more micropores formed in the polymeric coating layer as the moisture content of ZrO_2 nanoparticles increased. It seems that the phase inversion reaction can be facilitated by increasing the amount of moisture adsorbed onto the ZrO_2 nanoparticles.

To understand the change in the porosity caused by micropore formation, the porosity was determined by weighing the ZrO_2-composite separators with and without 1-butanol and using the following equation (3):

$$Porosity = m_a/\rho_a/(m_a/\rho_a + m_p/\rho_p) \tag{3}$$

Here, m_a and m_p are the weight of the ZrO_2-composite separators before and after impregnation of 1-butanol, respectively, and ρ_a and ρ_p are the density of 1-butanol and the dried ZrO_2 composite separators, respectively. It can be clearly observed that the porosity drastically increased with increasing moisture content. Similar behavior was observed in regard to electrolyte uptake (Fig. 4a). This result provides further evidence for the formation of a large amount of micropores in the polymeric coating layer as moisture content of ZrO_2 nanoparticles increased.

The corresponding air permeability and ionic conductivity of the composite separators are shown in Fig. 4b. As the ZrO_2 nanoparticle moisture content increased, a gradual decrease in the air permeability and an increase in the ionic conductivity of the ZrO_2-composite separator was observed. In particular, the air permeability and ionic conductivity obtained from the composite separator prepared using highly moisturized ZrO_2 nanoparticles (16000 ppm) were comparable to those of the pristine PE (i.e., without any ZrO_2 nanoparticles) separators. These results were consistent with the aforementioned observations on the microstructure of the ZrO_2-composite separators (Fig. 3).

Fig. 5 compares the electrochemical performance of LIBs using different ZrO_2-composite separators. It is evident that the capacity retention of cells employing ZrO_2-composite separators is highly dependent on the moisture content of ZrO_2 nanoparticles above 1 C. The achieved capacity is proportional to the increase in the moisture content because of the increased amount of micropores in the ZrO_2-composite separators (Fig. 5a). In particular, the cell assembled with the ZrO_2-composite separator prepared with highly moisturized ZrO_2 nanoparticles (16000 ppm) exhibited the same rate capability as that of the cell containing the pristine PE separator. It is likely that the highly moisturized ZrO_2 nanoparticles boosted the micropore formation and made the polymeric coating layer more porous. Fig. 5b shows cycle performance of the cells assembled with the pristine PE and ZrO_2-composite separators. All cells exhibited good capacity retentions (more than 96 % of their initial capacities) after 50 cycles. Interestingly, we found that the cells assembled with the ZrO_2-composite separators exhibited slightly higher capacity retentions than the cell with a pristine PE separator (in inset of Fig. 5b). According to literatures, the better electrolyte uptake ability of separator is more beneficial to prevent lack or leak of electrolyte during repeated cycling, resulting in enhancement of cycle performance.[8,17] Therefore,

11

we can conclude that the electrolyte uptake and ionic conductivity of the ZrO_2-composite separator can be enhanced by the formation of micropores, which offers better capacity retentions in LIBs during cycles.

Further, we examined the thermal stability of the proposed ZrO_2-composite separators. They were stored at the high temperatures of 120 °C and 150 °C for 1 h and then their thermal shrinkage was measured. These results are shown in Fig. 6. Compared to the pristine PE separator, the thermal shrinkage of the ZrO_2-composite separators was drastically reduced at 120 °C by incorporating ZrO_2 nanoparticles regardless of their moisture content. This becomes more obvious at the higher temperature of 150 °C. Addition of ZrO_2 nanoparticles is the main cause of this improvement.[17-19] Fig. 6b shows DSC profiles of the ZrO_2-composite separators in which an endothermic peak associated with the melting of PE was clearly observed in the temperature range between 120 and 150 °C. The pristine PE separator exhibited an onset temperature of 122.8 °C and melting temperature of 134.8 °C, respectively. Interestingly, ZrO_2-composite separators showed slightly higher onset and meting temperatures than those of the pristine PE separators (Table 2), which indicates that thermal stability of the composite separators can be enhanced by incorporation of ZrO_2 nanoprticles because they act as a heat-resistance material in the polymeric coating layer. It can therefore be concluded that the composite separator containing moisturized ZrO_2 nanoparticles is much more stable at high temperatures than the pristine PE separator without a deterioration in electrochemical performance.

CONCLUSION

12

We propose a ZrO$_2$-composite separator prepared by coating moisturized ZrO$_2$ nanoparticles with a PVDF-12wt%HFP copolymer binder. We investigated the correlation between the moisture content of the ZrO$_2$ nanoparticles and the microstructure of the polymeric coating layer in the proposed composite separators. As the moisture content increased, the number of micropores formed around the embedded ZrO$_2$ nanoparticles increased, thereby significantly affecting the electrochemical properties of the separators. When highly moisturized ZrO$_2$ nanoparticles (16000 ppm) were used to prepare the composite separators, adequate air permeability and ionic conductivity were attained. The electrochemical performance of the cell employing the highly moisturized ZrO$_2$-composite separator (16000 ppm) was comparable to that of the cell with a pristine PE separator. Moreover, the thermal stability can be effectively enhanced. Our findings will be helpful in the development of promising ceramic composite separators with excellent thermal and electrochemical properties.

ACKNOWLEDGMENTS

REFERENCES

1   Y. K. Sun, S. T. Myung, B. –C. Prakash, L. Belharouak, K. Amine, *Nat. Mater.,* 2009, **8**, 320.

13

2   N. Takami, H. Inagaki, T. Kishi, Y. Harada, Y. Fujita, K. Hoshina, *J. Electrochem. Soc.,* 2009, **156**, A128.

3   S. S. Zhang, K. Xu, T. R. Jow, *J. Power Sources,* 2003, **113**, 166.

4   H. Nakagawa, Y. Fujino, S. Kozono, Y. Katayama, T. Nukuda, H. Sakaebe, H. Matsumoto, K. Tatsumi, *J. Power Sources,* 2007, **174**, 1021.

5   P. Arora, Z. Zhang, *Chem. Rev.,* 2004, **104**, 4419.

6   G. Venugopal, J. Moore, J. Howard, S. Pendalwar, *J. Power Sources,* 1999, **77**, 34.

7   P. P. Prosini, P. Villano, M. Carewska, *Electrochim. Acta,* 2002, **48**, 227.

8   D. Takemura, S. Alhara, K. Hamano, M. Kise, T. Nishimura, H. Urushibata, H. Yoshiyasu, *J. Power Sources,* 2005, **146**, 779.

9   S. S. Zhang, K. Xu, T. R. Jow, *J. Power Sources,* 2005, **140**, 361.

10   Z. Li, G. Su, X. Wang, X. Li, *Electrochim. Acta,* 2004, **49**, 4633.

11   M. L. Yeow, Y. T. Liu, K. Li, *J. Appl. Polym. Sci.,* 2003, **90**, 2150.

12   W. Pu, X. He, L. Wang, C. Jiang, C. Wan, *J. Membrane Sci.* 2006, **272**, 11.

13   A. M. Stephan, D. Teeters, *Electrochim. Acta,* 2003, **48**, 2143.

14   Y. J. Hwang, K. S. Nahm, T. P. Kumar, A. M. Stephan, *J. Membr. Sci.,* 2008, **310**, 349.

15   B. Chu, M. Lin, B. neese, Q. Zhang, *J. Appl. Phys.,* 2009, **105**, 014103.

16   PH. Vermeiren, R. Leysen, H. Beckers, J. P. Moreels, A. Claes, *J. Porous Mat.,* 2008, **15**, 259.

17   J. −A. Choi, S. H. Kim, D. −W. Kim, *J. Power Sources,* 2010, **195**, 6192.

18   H. -S. Jeong, J. H. Noh, C. −G. Hwang, S. H. Kim, S. −Y. Lee, *Macromol. Chem. Phys.,* 2010, **211**, 420.

19   H. −S. Jeong, S. C. Hong, S. −Y. Lee, *J. Power Sources,* 2010, **364**, 177.

TABLES

Table 1. Physical properties of ZrO$_2$ nanoparticles.

Items	Value
Purity (%)	99.9 (Metal basis excluding Hf, Hf < 3 wt%)
Crystal phases	Monoclinic
Particle size (nm)	40–50
Specific Surface Area (m^2 g^{-1})	20–30
Bulk density (g cm^{-3})	0.4–0.5
True density (g cm^{-3})	5.89

Table 2. Onset and melting temperature of the ZrO$_2$-composite separators measured by DSC analysis.

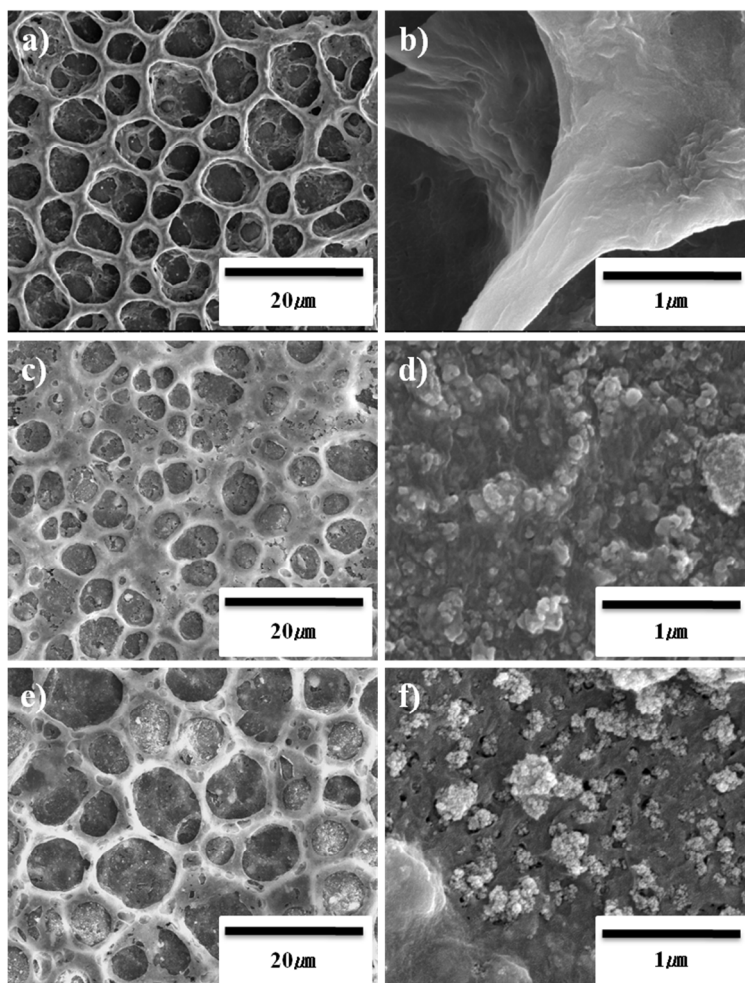| Samples	Onset temperature (^{o}C)	Melting temperature (^{o}C)
PE	122.8	134.8
100	128.1	136.2
3000	128.9	138.5
6000	128.2	137.4
15000	129.0	137.3
16000	129.0	138.6

FIGURES

Fig. 1. FESEM images of the composite separators with different coatings at different magnifications. (a) A separator coated with only PVDF-12wt%HFP copolymer. (b) The same separator at 1μm. (c) A composite separator coated in PVDF-12wt%HFP copolymer and dried ZrO_2 nanoparticles 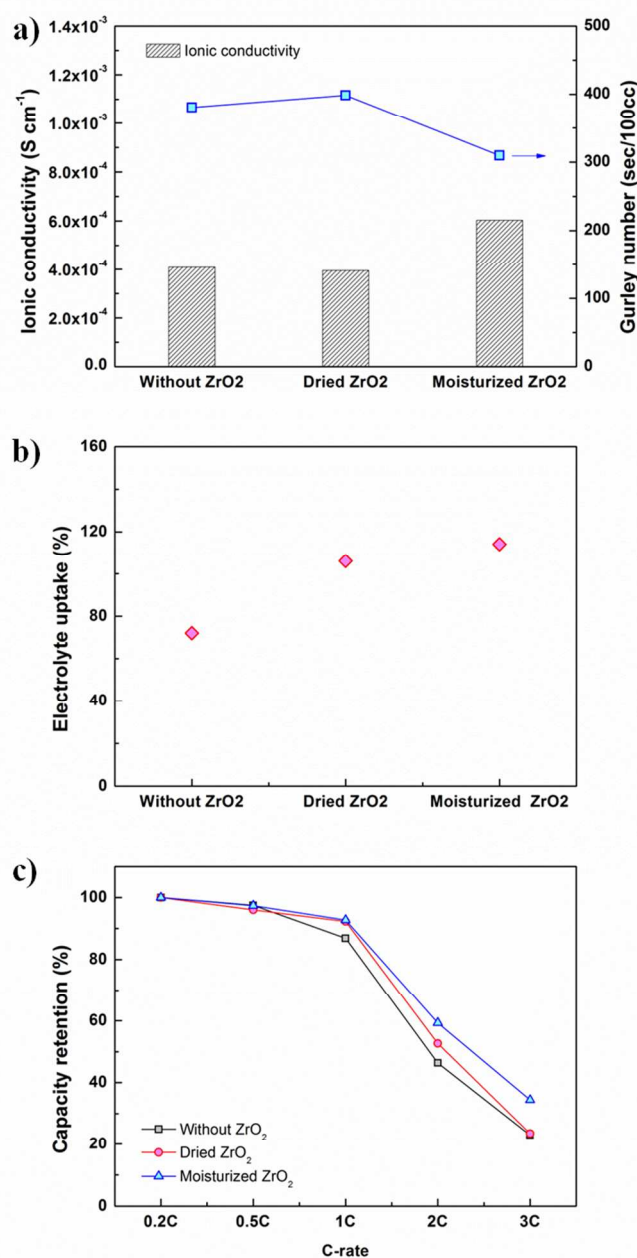(moisture content : 100 ppm). (d) The same separator at 1μm. (e)　A composite separator coated in PVDF-12wt%HFP copolymer and moisturized ZrO_2 nanoparticles (moisture content : 3000 ppm). (f) The same separator at 1μm.

17

Fig. 2. (a) Ionic conductivity and air permeability, and (b) electrolyte uptake of the composite separators coated with only PVDF-12wt%HFP copolymer, with dried ZrO_2 nanoparticles, or moisturized ZrO_2 nanoparticles. (c) A comparison of the rate capabilities of LIBs assembled using the composite separators. The cells were charged and discharged in a voltage range of 3.0–4.2 V *vs.* Li/Li$^+$ at different currents of 0.2, 0.5, 1.0, 2.0 and 3.0 C (1 C = 150 mA g^{-1}).
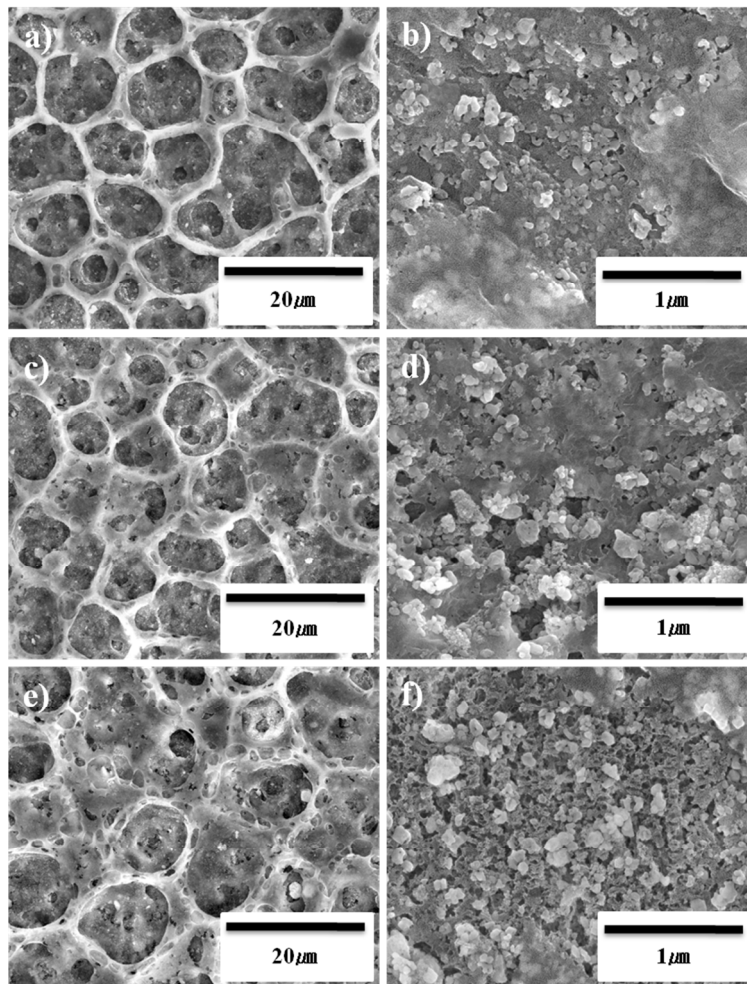
18

Fig. 3. (a), (b) FE-SEM images of the composite separator coated with PVDF-12wt%HFP copolymer and moisturized ZrO_2 nanoparticles (moisture content : 6000 ppm). (c), (d) FESEM images of the composite separator coated with PVDF-12wt%HFP and moisturized ZrO_2 nanoparticles (moisture content : 15000 ppm). (e), (f) FESEM images of the composite separator coated with PVDF-12wt%HFP copolymer and moisturized ZrO_2 nanoparticles (moisture content : 16000 ppm) at different magnifications.
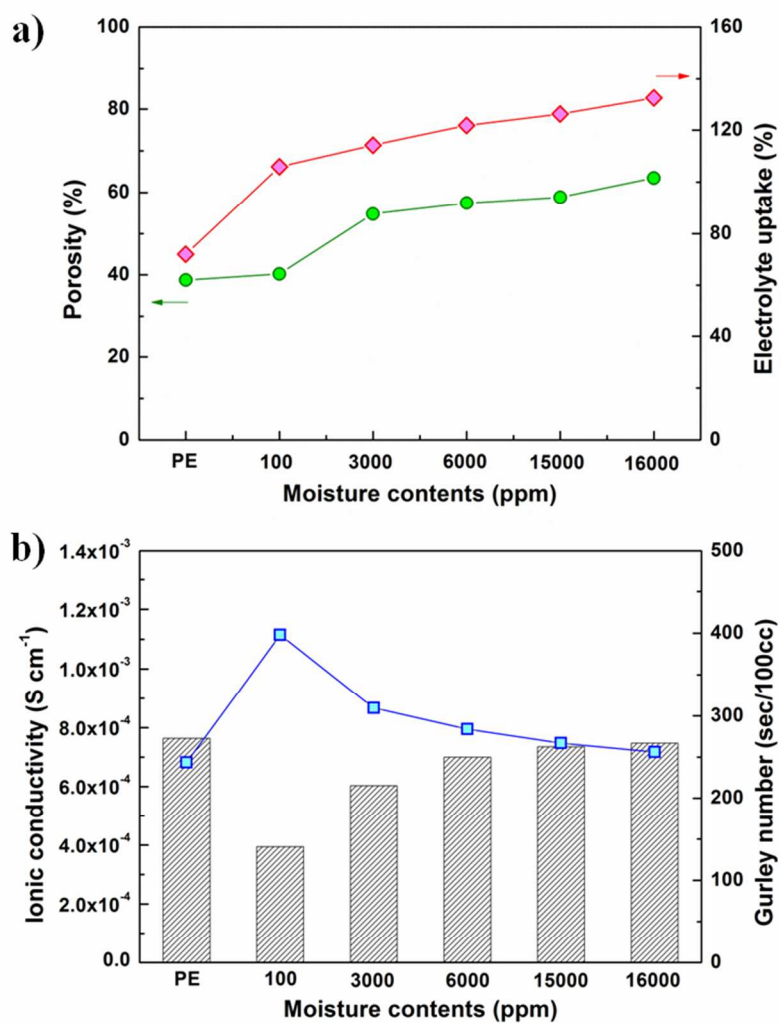
Fig. 4. (a) Porosity and electrolyte uptake of the composite separators coated with PVDF-12wt%HFP copolymer with various moisturized ZrO_2 nanoparticles. (b) Ionic conductivity and air permeability of the composite separator coated with PVDF-12wt%HFP copolymer with various moisturized ZrO_2 nanoparticles.
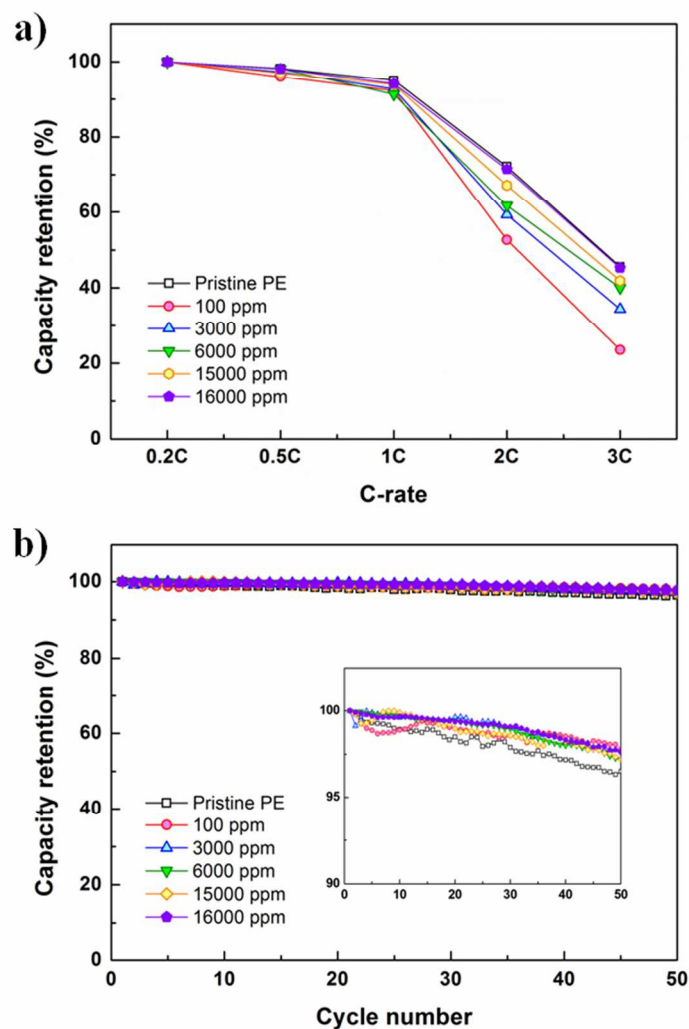
20

Fig. 5. (a) Comparisons of the rate capabilities of LIBs assembled using the composite separators. The cells were charged and discharged in a voltage range of 3.0–4.2 V *vs.* Li/Li$^+$ at different currents of 0.2, 0.5, 1.0, 2.0 and 3.0 C (1 C = 150 mA g^{-1}). (b) Cyclic performance of LIBs assembled with the composite separators. The cells were charged and discharged in a voltage range of 3.0–4.2 V *vs.* Li/Li$^+$ at constant current of 0.5 C.
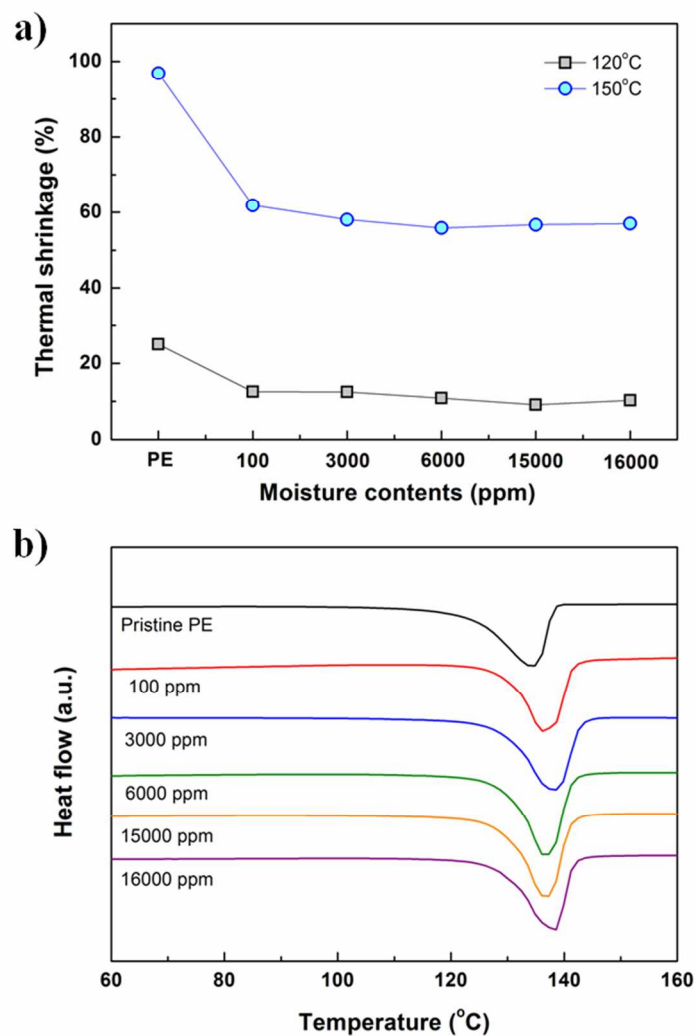
Fig. 6. (a) Comparison of thermal shrinkages of the composite separators coated with PVDF-12wt%HFP copolymer with various moisturized ZrO_2 nanoparticles at 120 ^{o}C (■) and 150 ^{o}C (●). (b) DSC profiles of the composite separators prepared with various moisturized ZrO_2 nanoparticles.

.